Biomedicine & Pharmacotherapy 144 (2021) 112307

Contents lists available at ScienceDirect

Biomedicine & Pharmacotherapy

journal homepage: www.elsevier.com/locate/biopha

Preclinical toxicological study of long-circulating and fusogenic liposomes co-encapsulating paclitaxel and doxorubicin in synergic ratio

Marjorie Coimbra Roque [a], Caroline Dohanik da Silva [a], Marthin Raboch Lempek [b], Geovanni Dantas Cassali [c], André Luís Branco de Barros [a], Marília Martins Melo [b], Mônica Cristina Oliveira [a,*]

[a] Department of Pharmaceutical Products, Faculty of Pharmacy, Universidade Federal de Minas Gerais, Belo Horizonte, Minas Gerais, Brazil
[b] Department of Veterinary Clinic and Surgery, Faculty of Veterinary Medicine, Universidade Federal de Minas Gerais, Belo Horizonte, Minas Gerais, Brazil
[c] Department of General Pathology, Institute of Biological Sciences, Universidade Federal de Minas Gerais, Belo Horizonte, Minas Gerais, Brazil

ARTICLE INFO

Keywords:
Liposomes
Doxorubicin
Paclitaxel
Co-administration
Acute toxicity
Breast cancer

ABSTRACT

Combination therapy between paclitaxel (PTX) and doxorubicin (DXR) is applied as the first-line treatment of breast cancer. Co-administration of drugs at synergistic ratio for treatment is facilitated with the use of nanocarriers, such as liposomes. However, despite the high response rate of solid tumors to this combination, a synergism of cardiotoxicity may limit the use. Thus, the objective of this work was to investigate the toxicity of long-circulating and fusogenic liposomes co-encapsulating PTX and DXR at the synergistic molar ratio (1:10) (LCFL-PTX/DXR). For this, clinical chemistry, histopathological analysis and electrocardiographic exams were performed on female Balb/c mice that received a single intravenous dose of LCFL-PTX/DXR. The results of the study indicated that the LD50 dose range (lethal dose for 50% of animals) of the LCFL-PTX/DXR treatment (28.9–34.7 mg/kg) is much higher than that found for free PTX/DXR treatment (20.8–23.1 mg/kg). In addition, liposomes promoted cardiac protection by not raising CK-MB levels in animals, keeping cardiomyocytes without injury or electrocardiographic changes. After 14 days of treatment, free PTX/DXR caused prolongation of the QRS interval when compared to LCFL-PTX/DXR treatment at the same dose (37.0 ± 5.01 ms and 30.83 ± 2.62 ms, respectively, with $p = 0.017$). The survival rate of animals treated with LCFL-PTX/DXR was three times higher than that of those treated with free drugs. Thus, it was established that the toxicity of LCFL-PTX/DXR is reduced compared to the combination of free PTX/DXR and this platform has advantages for the clinical treatment of breast cancer.

1. Introduction

Cancer is one of the major health problems of the 21st century, and breast cancer is the most common malignancy in women. It is estimated that more than 23 million cases will be diagnosed by 2030 [1,2]. Currently, several therapeutic approaches are available, depending on the cancer subtype: surgery, hormonal therapy, radiation therapy, immunotherapy, and chemotherapy [2,3]. In the case of breast cancer chemotherapy, combined treatment with paclitaxel (PTX) and doxorubicin (DXR) is one of the most common approaches. The associated treatment is partly successful due to the synergistic effect between drugs, which presents different mechanisms of action overcoming drug resistance to a certain extent [4–7]. This synergism implies a greater effect of the combination compared to the effect of the sum of the individual drugs. This approach allows the therapeutic efficacy to be achieved with lower doses of the drugs, which consequently also brings a reduction of the side effects [8–11].

However, the systemic administration of the cocktail of bioactive substances does not guarantee that they reach the target together and in the appropriate concentration for synergism due to their own pharmacokinetics [11,12]. The need to control combinatorial ratios so that the synergistic ratio is reached in the body and delivered to the tumor site has led to the development of nanosystems co-encapsulating drugs in synergistic ratios [10,12,13].

Thinking about this theme, Roque and collaborators (2019) developed and characterized a formulation of long-circulating and fusogenic

* Correspondence to: Department of Pharmaceutical Products, Faculty of Pharmacy, Universidade Federal de Minas Gerais, P.O. Box: 31.270-901, Belo Horizonte, Minas Gerais, Brazil.
E-mail addresses: itabra2001@yahoo.com.br, monicacristina@ufmg.br (M.C. Oliveira).

https://doi.org/10.1016/j.biopha.2021.112307
Received 15 August 2021; Received in revised form 29 September 2021; Accepted 5 October 2021
Available online 13 October 2021

liposomes co-encapsulating PTX and DXR in the molar ratio 1:10 (LCFL-PTX/DXR) for the treatment of breast cancer. The formulation has chemical and physicochemical characteristics suitable for intravenous administration and is capable of co-encapsulating the drugs in the pre-established molar ratios. Besides LCFL-PTX/DXR showed to be stable for 30 days, maintaining their size characteristics (244.4 ± 28.1 nm), polydispersity index (PI) (0.29 ± 0.01), zeta potential (PZ) (− 4.97 ± 0.64 mV), and drug retention content (74.0 ± 2.0% for PTX and 89.6 ± 12.3% for DXR). Thus, in this work we investigated the step of the preclinical evaluation of a new pharmaceutical formulation related to the toxicological study. The lack of data related to the effect of the simultaneous administration of DXR and PTX in healthy individuals led us to develop studies of toxicity of LCFL-PTX/DXR. In addition, toxicity studies are an important step when the aim is to introduce new pharmaceutical products for clinical use [14,15]. Preclinical toxicological tests allow a scientific basis to predict the main side effects and the consequences of an overdose for further escalation in humans [16].

2. Materials and methods

2.1. Materials

1,2-Dioleoyl-sn-glycero-3-phosphoethanolamine (DOPE) and 1,2 distearoyl-*sn*-glycero-3-phosphoethanolamine-N-[amino(poly-ethyleneglycol) 2000 (DSPE-PEG_{2000}) were supplied by Lipoid GmbH (Ludwigshafen, Germany). Cholesterol hemisuccinate (CHEMS), doxorubicin (DXR), 4-(2-hydroxyethyl)-1-piperazineethanesulfonic acid (HEPES) sodium salt, sodium chloride, sodium hydroxide and Cremophor EL were obtained from Sigma-Aldrich Co. (St Louis, MO, USA). Paclitaxel (PTX) was supplied by Quiral Quimica do Brasil S.A (Juiz de Fora, Brazil). All other chemicals used in this study were of analytical grade. The female Balb/c mice were obtained from Centro de Bioterismo (CEBIO/UFMG, Belo Horizonte, Brazil) and the treatments to which they were submitted were approved by Comissão de Ética no Uso de Animais (CEUA/ UFMG, Belo Horizonte, Brazil) under the protocol number 39/2019.

2.2. Liposome preparation

LCFL-PTX/DXR was prepared by the lipid film hydration technique using a rotary evaporator Buchi Labortechnik AG CH-9233, model R-210, coupled to a V-700 vacuum pump (Flawil, Switzerland). For this, chloroform aliquots of DOPE, CHEMS, and DSPE-PEG_{2000} (total lipid concentration equal to 10 mM, molar proportions equal to 5.7: 3.8: 0.5, respectively) and PTX (concentration equal to 0.25 mg/mL) were transferred to a round bottom flask and subjected to evaporation in a water bath at 50 °C to remove the solvent. The lipid film obtained was then kept for 1 h under an atmosphere of chloroform for better dispersion of PTX in the lipids, according to the technique known as annealing [17].

An aliquot of the 0.1 M NaOH solution was added to the film to promote complete ionization of CHEMS, and the subsequent formation of a lamellar structure. The lipid film was hydrated with a solution of ammonium sulfate (300 mM, pH 7.4) preheated in a 50 °C water bath. The mixture was kept in the ultrasonic bath for 10 min to hydrate the lipid film. The non-encapsulated PTX was then separated from the liposomes by centrifugation at 3000 rpm, at 25 °C, for 10 min (Heraeus Multifuge X1R centrifuge, Thermo Fischer Scientific, Massachusetts, USA). To remove the non-encapsulated ammonium sulfate, the liposomes were kept on dialysis for 24 h against HEPES buffered saline solution (HBS), pH 7.4. The concentration of PTX in these liposomes was determined by high performance liquid chromatography (HPLC).

After determining the PTX concentration, a super concentrated solution of DXR (34 mg/mL) was incubated with the liposomes to obtain a 1:10 molar ratio of PTX and DXR respectively. DXR encapsulation was performed by remote loading, conducted by a gradient of transmembrane sulfate. The liposomes containing PTX were kept in contact with DXR for 2 h at 25 °C, and then dialyzed against HEPES buffered saline solution (HBS), pH 7.4, for 24 h, to remove unencapsulated DXR [6].

2.3. Determination of the content of PTX and DXR in LCFL-PTX/DXR

To determine the encapsulation percentage of the drugs in LCFL-PTX/DXR, chromatography and spectrometry methods were used. The concentration of PTX was measured using the chromatograph composed of a Model 515 pump, a Model 717 Plus autoinjector, and a Model 2996 DAD detector (Waters Instruments, Milford, USA), controlled by Empower software, version 2.0. The liposomal vesicles were disrupted using isopropyl alcohol in a volume ratio of 1:2 and later diluted in a mixture of acetonitrile:water (55:45 v/v). This dispersion was filtered through a 0.45 μm Millex HV filter (Millipore, Billerica, MA, USA) and injected in the chromatographic apparatus. For analysis, a Hibar 250-4 LiChrospher 100RP-18, 25 cm × 4 mm, 5 μm column (Merck, Darmstadt, Germany) was used. The eluent system consisted of acetonitrile:water (55:45) in a flow equal to 1.2 mL/min. The injection volume was 10 μL and the running time was 8 min. The eluate was detected at a wavelength equal to 227 nm at room temperature [18]. The PTX encapsulation percentage (EP) was calculated according to the following equation:

$$EP = \frac{[\text{amount of PTX in purified liposomes}] \times 100}{[\text{amount of PTX in non} - \text{purified liposomes}]}$$

UV–VIS spectrophotometry (Thermo evolution 201 UV visible spectrophotometer) was used as the method for quantification of DXR in the liposomes. The analyzes were performed evaluating the absorbance at a wavelength equal to 480 nm [19]. Regression equation and linearity (r^2) were $y = 0.01814x + 0.01119$ and 0.997, respectively. The accuracy was found to be between 98% and 104% ($n = 3$) and samples of blank liposomes showed no absorbance at the wavelength used [6]. Initially, the vesicles were opened with isopropyl alcohol at a ratio of 1:2, respectively, and then the preparations were diluted in HEPES buffered saline (HBS), pH 7.4. The DXR encapsulation percentage (EP) was calculated according to the following equation:

$$EP = \frac{[\text{amount of DXR in purified liposomes}] \times 100}{[\text{amount of DXR in non} - \text{purified liposomes}]}$$

2.4. Determination of size, polydispersity index, and zeta potential of LCFL-PTX/DXR

The diameter of the vesicles and the polydispersity index (PI) were determined by dynamic light scattering (DLS). The measurements were performed at a temperature of 25 °C, using a 90° laser incidence angle. The zeta potential (ζ) of the vesicles was determined by DLS associated with electrophoretic mobility. To perform all measurements, 30 μL of liposomes was diluted in 1 mL of HEPES buffered saline (HBS), pH 7.4, and evaluated on the Zetasizer Nano ZS90 equipment (Malvern, England).

2.5. Acute toxicity study

The assessment of acute toxicity *in vivo* was carried out according to the recommendations of the Organization for Economic Cooperation and Development (OECD) 423 [20], adapted for formulations for parenteral use. It is worth mentioning that the OECD standards were established for an acute toxicity study after administration of the substances orally, with the recommended doses equal to 5, 50, 300, and 2000 mg/kg. Considering the intravenous administration route, the initial dose proposed in this study was 20.8 mg/kg of the total drugs (PTX + DXR) administered. In previous studies, our research group found that the maximum tolerated dose of DXR encapsulated in

liposomes composed by DOPE, CHEMS, and DSPE-PEG2000 (5.8: 3.7: 0.5 molar ratio, respectively) was greater than 15 mg/kg [21]. Therefore, based on this study, we chose to use 18 mg/kg of DXR and 2.8 mg/kg of PTX to get a 1:10 molar ratio, respectively.

The parameters evaluated for the determination of toxicity were behavioral observation, body weight, water and feed consumption, mortality, biochemical and hematological analysis, histopathological evaluation, and electrocardiographic analysis. The experimental model adopted was healthy female Balb/c mice aged between 8 and 9 weeks and weighing approximately 20 g. The animals were divided into 8 groups and the treatments received by the groups were NaCl 0.9% (w/v) solution (saline), free PTX/DXR, and LCFL-PTX/DXR in different dosages, as shown in Table 1.

In all groups, the formulations were administered in a single dose intravenously (tail vein) and the animals were observed daily for a period of 14 days. The mice were weighed and the water and feed consumption evaluated every 3 days. After the observation period, the animals were anesthetized with a mixture of ketamine (80 mg/kg) and xylazine (15 mg/kg) intraperitoneally. The blood was collected by puncture of the brachial plexus for hematological and biochemical exams.

Initially, each group was composed of 3 animals. If the tested dose was able to cause death in 2 or more animals of the group, it was considered that the LD50 by the animals was lower than the tested one. Therefore, it was necessary to start new tests at a lower dose, according to the OECD guidelines. However, when the assessed dose caused one or no death, the recommendation followed was to repeat the observations with 3 animals using the same dose. Thus, each group consisted of 6 animals. Confirmation of the results it meant that the tested dose was not yet the LD50, and the OECD guidance recommends continuing the study with a new group using a higher dose. The figure with the treatment scheme used to assess acute toxicity in this work is in the Appendix A.

2.6. Hematology and biochemistry analysis

For hematological analysis, the animal blood was collected in tubes containing the anticoagulant (EDTA 0.1M) and inserted into the automated hematological analyzer HEMOVET 2300 (Hemovet, São Paulo, Brazil). Hematological parameters related to hematocrit, erythrocytes, hemoglobin and also white blood cells were evaluated for each group.

For biochemical analysis, the blood was centrifuged (3000 rpm, 15 min) and the plasma obtained was collected. The tests were carried out on the Bioplus BIO-2000 semiautomatic analyzer (Bioplus, São Paulo, Brazil) using commercial kits (Labtest, Lagoa Santa, Brazil). Renal function was assessed by measuring urea and creatinine; liver function by determining the activity of alanine aminotransferase (ALT) and aspartate aminotransferase (AST); and cardiac injury by measuring the creatine kinase activity – (CK-MB).

2.7. Histology

Liver, kidneys, sternum, spleen, lungs, and heart were collected for histopathological analysis. Samples were fixed in phosphate-buffered formalin 10% (pH = 7.4) for 24–48 h, dehydrated in alcohol, and included in paraffin blocks. 4 μm sections were obtained and stained with hematoxylin and eosin. The slides were evaluated by trained pathologists and images were captured by a camera connected to an optical microscope (Olympus BX-40; Olympus, Tokyo, Japan).

2.8. Electrocardiographic analysis

In order to obtain the electrocardiograms (ECG), all animals were anesthetized with closed loop inhalation anesthesia (VetCase®, Sumare, São Paulo, Brazil) with isoflurane (Isoflurine® 2.5% for induction and 1.5% for maintenance). ECG monitoring (ECG-PC VET, Tecnologia Eletrônica Brasileira SA – TEB®, São Paulo, Brazil) was maintained for 1 min after stabilization. The animals were placed in the supine position and the electrodes were placed on the thoracic and pelvic limbs. Heart rate, duration, amplitude, and interval of electric waves were evaluated. The experimental groups evaluated were animals treated with the LD50 lower limit dose of the combination of free PTX/DXR (20.8 mg/kg), determined in the previous acute toxicity study. As a counterpoint, the group treated with the formulation LCFL-PTX/DXR, at the same concentration, was also evaluated. In addition, the electrocardiograms of mice that received the LD50 lower limit dose for liposomes (28.9 mg/kg) were observed. The following parameters were analyzed: QT interval (measured from the beginning of the QRS complex to the end of the T-wave), ST interval (measured from the end of QRS complex to beginning of T-wave),QRS complex (measured from the beginning of the Q-wave to the end of the S-wave) and the RR interval (interval between two successive R-waves and used for the determination of heart rate HR = 60/RR). QT interval was corrected by HR using Fridericia's formula ($QTc = QT/(RR)^{1/3}$) [21,22].

3. Statistical analysis

The normality and homoscedasticity of the variables were verified by the Shapiro-Wilk and Brown-Forsythe tests, respectively. Regarding the analysis of the treatments, the One-way ANOVA test with Tukey's post-test was used to verify if the means of the groups differed significantly. If the data were not normal or homoscedastic, the Kruskal-Wallis test with Dunn's post-test was used for the same purpose. The Two-way ANOVA test with Tukey's post-test was also used to relate two different independent variables over one dependent variable. Values of $p < 0.05$ were considered significant. The analyzes were performed using the GraphPad Prism software (version 9.00, La Jolla, California, USA).

4. Results

4.1. Preparation and characterization of LCFL-PTX/DXR

LCFL-PTX/DXR followed the pattern developed by Roque et al. [6], co-encapsulating PTX and DXR in the 1:10 synergistic molar ratio, maintaining an adequate diameter close to 200 nm with low polydispersity and slightly negative zeta potential, but close to neutrality as shown in Table 2.

4.2. Acute toxicity study

4.2.1. Evaluation of animal mortality and morbidity

The evaluation of the LD50 by the animals of the PTX/DXR drug combination (molar ratio 1:10 respectively) started with 20.8 mg/kg (2.8 mg/kg PTX + 18 mg/kg DXR), both for the combination of free drugs and for the LCFL-PTX/DXR formulation. For the combination of free drugs at this dose, marked piloerection was observed in all animals, with the presence of signs of diarrhea and ascites in one of them. For the first 3 mice evaluated, there was only 1 death on the 9th day of the

Table 1
Physicochemical characteristics of LCFL-PTX/DXR.

[PTX] mg/mL	[DXR] mg/mL	DXR/PTX molar ratio	Mean diameter (nm)	PI	Zeta potential (mV)
0.15 ± 0.02	0.96 ± 0.28	10.10 ± 1.81	211.8 ± 16.3	0.29 ± 0.02	-7.39 ± 2.20

PTX: paclitaxel; DXR: doxorubicin; PI: polydispersity index. The results are presented as mean ± standard deviation from the mean (n = 10).

Table 2
Experimental groups evaluated in acute toxicity studies for biochemical, hematological analysis and observations of mortality and morbidity.

Formulation	Groups	Dosage of drug (mg/kg)		Total dose of drugs (mg/kg)
		PTX	DXR	
Free PTX/DXR	1	2.8	18	20.8
	2	3.1	20	23.1
LCFL-PTX/DXR	3	2.8	18	20.8
	4	3.1	20	23.1
	5	3.4	22	25.4
	6	3.9	25	28.9
	7	4.7	30	34.7
Control (saline)	8	–	–	–

study. According to the experimental planning shown in the Appendix A, this step was repeated with three more animals, and we verified one death on the 12th day of the experiment. Thus, according to the OECD 423 guideline, a higher dose of the combination of free drugs should be tested. The dose of 23.1 mg/kg (3.1 mg/kg PTX + 20 mg/kg DXR) was injected in mice. After 3 days of application of the drugs, piloerection and lethargy of the animals were observed, resulting in 2 deaths on the 7th day of the study. Therefore, according to OECD 423 rules, the LD50 for free PTX/DXR treatment in the 1:10 molar ratio is between 20.8 and 23.1 mg/kg for this experimental model. Thus, 23.1 mg/kg was the last dose tested for the combination of free drugs.

The studies with LCFL-PTX/DXR also started with a dose of 20.8 mg/kg and due to the absence of deaths or morbidities, they evolved by a higher number of tested doses, as shown in Table 1 and the diagram in the Appendix A. For this treatment, up to a dose of 28.9 mg/kg (3.9 mg/kg PTX + 25 mg/kg DXR), no death was observed. However, for the doses of 25.4 mg/Kg (3.4 mg/kg PTX + 22 mg/kg DXR) and 28.9 mg/kg (3.9 mg/kg PTX + 25 mg/kg DXR) there was loss of weight of the animals varying between 8% and 10% in the first 3 days after administration of LCFL-PTX/DXR. However, in the following days the recovery of the weight occurred. For the dose of 28.9 mg/kg, mild piloerection and the formation of mild to moderate ascites were seen in most of these animals.

According to these results, we repeated the experiments for each group treated with LCFL-PTX/DXR at doses of 20.8, 23.1, 25.4 and 28.9 mg/kg using 3 more animals per treatment, and the observations were confirmed. It was concluded that the treatment with doses higher than 20.8 mg/kg of the drugs PTX and DXR was only possible with the use of liposomes, since no morbidity and mortality were seen in the animals.

We followed the acute toxicity study for LCFL-PTX/DXR treatment, increasing the dose to 34.7 mg/kg (4.7 mg/kg PTX + 30 mg/kg DXR). However, it was necessary to interrupt the study and sacrifice the animals on the 4th day after intravenous administration of the formulation. Severe signs of morbidity were detected, such as intense weight loss reaching 15%, piloerection, signs of diarrhea, and cyanotic tail. After desiccation of the animals, the intestines were found dilated with accumulation of feces. Thus, the LD50 for LCFL-PTX/DXR treatment was the doses range equivalent to 28.9–34.7 mg/kg of drugs.

4.2.2. Hematological analysis

The results for the hematological exams are shown in Table 3. The hematological examination revealed no changes in the distribution of red blood cells (RDW). However, hematocrit (HCT), the amount of hemoglobin per blood volume (HGB), and the number of red blood cells (RBC) showed a slight reduction for groups treated with higher concentrations of drugs in liposomes (23.1, 25.6, and 28.9 mg/kg).

The evaluation of white blood cells showed that the amount of granulocytes (neutrophils, eosinophils and basophils) increased the LCFL-PTX/DXR treated group with the highest doses (23.1, 25.6 and 28.9 mg/kg). However, the amount of agranulocytes (lymphocytes and monocytes) decreased in these same groups, when compared to the control group. This opposite behavior resulted in the maintenance of the total white blood cell count (WBC) equal to the control group. The other groups evaluated as free PTX/DXR and LCFL-PTX/DXR (20.8 and 23.12 mg/kg) also had no significant difference in WBC values compared to the control group.

The amount of platelets (PLT) increased significantly with the increase of the dosage of the LCFL-PTX/DXR treatment administered to mice. This increase appears to be the result of a reactive thrombocytosis, a clinical disorder that stimulates the bone marrow to produce excess platelets.

4.2.3. Biochemical analysis

The results for the biochemical analysis are shown in Table 4. It was observed that the doses used did not cause changes in renal function, since there was no significant difference in the concentration of urea and creatinine between the groups when compared to the control.

Increased serum levels of ALT and AST may indicate the development of drug-induced acute liver injury in animals [21,23]. In this study, serum ALT levels for all groups treated with LCFL-PTX/DXR, regardless of the dose administered (20.8, 23.1, 25.4, or 28.9 mg/kg), were equal to those determined for the group treated with free PTX/DXR (20.8 mg/kg) at the dose equivalent to the lowest administered in liposomes. In addition, the groups treated with LCFL-PTX/DXR (23.1, 25.4, and 28.9 mg/kg), including the highest dose tested, had serum ALT levels equivalent to the control group. This confirms that liposomal formulations at the doses cited are not capable of producing sufficient liver toxicity to elevate ALT. On the other hand, the AST enzyme serum levels showed to be high for all treatments performed with LCFL-PTX/DXR (20.8, 23.1, 25.4, or 28.9 mg/kg) compared to the control group. The CK-MB enzyme cardiotoxicity marker level presented elevated only for the group treated with LCFL-PTX/DXR at the dose of 25.4 mg/kg, which stood out from the others.

Table 3
Hematological parameters for Balb/c mice treated with different doses of LCFL-PTX/DXR and one free combination of PTX and DXR.

Blood components	Control	Free PTX/DXR 20.8 (mg/kg)	LCFL-PTX/DXR (mg/kg)			
			20.8	23.1	25.4	28.9
WBC (cel mm3 x 103)	4.78 ± 1.34^{a}	6.93 ± 1.29^{a}	5.50 ± 1.27^{a}	4.55 ± 2.08^{a}	6.92 ± 1.82^{a}	4.55 ± 1.72^{a}
NON GRANULOCYTES (%)	67.53 ± 2.73^{a}	63.73 ± 10.42^{ab}	53.22 ± 8.95^{abc}	51.25 ± 10.68^{bc}	47.58 ± 11.72^{bc}	42.47 ± 6.81^{c}
GRANULOCYTES (%)	32.47 ± 2.73^{a}	36.27 ± 10.42^{ab}	46.78 ± 8.95^{abc}	48.75 ± 10.68^{bc}	52.42 ± 11.72^{bc}	57.53 ± 6.81^{c}
RBC (%)	6.67 ± 0.18^{a}	6.01 ± 0.51^{ab}	6.37 ± 0.28^{ab}	5.86 ± 0.34^{b}	6.01 ± 0.46^{b}	5.83 ± 0.34^{b}
HGB (cel mm3 X 106)	12.95 ± 0.45^{a}	11.30 ± 1.45^{ab}	12.02 ± 0.72^{ab}	11.08 ± 0.87^{b}	11.23 ± 1.97^{b}	10.85 ± 0.72^{b}
HCT (%)	32.82 ± 1.45^{a}	30.07 ± 3.11^{ab}	31.53 ± 1.44^{ab}	29.00 ± 1.97^{b}	29.25 ± 2.49^{b}	28.03 ± 1.78^{b}
RDW (%)	14.20 ± 0.39^{a}	14.47 ± 0.40^{a}	14.77 ± 0.48^{a}	14.30 ± 0.17^{a}	14.67 ± 0.60^{a}	14.08 ± 0.39^{a}
PLT (cel mm3 x 103)	288.00 ± 27.34^{a}	271.50 ± 43.13^{ac}	448.20 ± 64.40^{b}	566.80 ± 79.68^{d}	478.00 ± 45.66^{bd}	396.60 ± 61.51^{bc}

WBC: means white blood cells; RBC: red blood cells; HGB: hemoglobin; HCT: hematocrit; RDW: red cell distribution width; PLT: platelet. The results are presented as mean ± standard deviation from the mean (n = 6). Different letters represent a significant difference between the parameters evaluated ($p < 0.05$). Data were evaluated by One-way ANOVA (Tukey's post-test), if they were abnormal, the Kruskal-Wallis test with Dunn's post-test was used.

Table 4
Biochemical parameters for Balb/c mice treated with different doses of LCFL-PTX/DXR and one free combination of PTX and DXR.

Biochemical parameters	Control	Free PTX/DXR 20.8 (mg/kg)	LCFL-PTX/DXR (mg/kg)			
			20.8	23.1	25.4	28.9
CREATININE (mg/dL)	0.36 ± 0.09^{a}	0.48 ± 0.19^{a}	0.37 ± 0.09^{a}	0.37 ± 0.13^{a}	0.42 ± 0.05^{a}	0.34 ± 0.08^{a}
UREA (mg/dL)	48.16 ± 4.65^{a}	49.47 ± 2.64^{ab}	46.11 ± 2.52^{ab}	36.03 ± 5.20^{b}	42.67 ± 6.24^{ab}	53.19 ± 10.08^{a}
ALT (U/L)	28.64 ± 2.79^{a}	32.88 ± 2.19^{ab}	57.10 ± 18.85^{b}	49.06 ± 14.83^{ab}	47.00 ± 16.81^{ab}	46.97 ± 12.04^{ab}
AST (U/L)	36.14 ± 7.90^{a}	67.22 ± 36.23^{ac}	126.90 ± 21.99^{b}	125.00 ± 28.96^{b}	105.50 ± 29.83^{bc}	91.23 ± 12.23^{bc}
CK-MB (U/L)	37.25 ± 9.33^{a}	53.58 ± 2.95^{ab}	45.55 ± 1.40^{ab}	55.64 ± 14.89^{ab}	70.01 ± 18.83^{b}	50.24 ± 17.27^{ab}

ALT: means alanine aminotransferase; AST: means aspartate aminotransferase; CK-MB: means creatine kinase MB isoform. The results are presented as mean- ± standard deviation from the mean (n = 6). Different letters represent a significant difference between the parameters evaluated ($p < 0.05$). Data were evaluated by One-way ANOVA (Tukey's post-test), if they were abnormal, the Kruskal-Wallis test with Dunn's post-test was used.

4.2.4. Histology

Histological analyses were performed with all groups evaluated in hematological and biochemical tests for both free drug and liposome treatments. Thus, the groups treated with the combination of free PTX/DXR in the total dose of 23.1 mg/kg and the group treated with LCFL-PTX/DXR in the total dose of 34.7 mg/kg were also desiccated and the organs and tissues were evaluated.

The analysis of cardiac tissues revealed that for treatments with free drugs at the (20.8 mg/kg) and at a higher dose (23.1 mg/kg), there was a start of vacuolization of cardiomyocytes, indicating discrete multifocal degeneration, which was not observed for treatments involving liposomes in any of the tested doses. Representative photomicrographs of the heart can be seen in Fig. 1**A–C**. Representative images of the control group **(A)** were placed from left to right, followed by free PTX/DXR treatments at doses of 20.8 **(B)** and 23.1 **(C)** mg/kg, in which the arrows indicate the presence of small cytoplasmic vacuoles in the cardiomyocytes.

The analysis of bone marrow showed changes only at the highest doses of liposomes administered (28.9 and 34.7 mg/kg), whose photomicrographs are shown in Fig. 1**D–F**. Photo **(D)** is representative of the control group, without histological changes. For 28.9 mg/kg, there was a reduction in cellularity **(E)** that evolved to severe hypocellularity in the higher dose of 34.7 mg/kg **(F)**.

The liver in all treatments presented mild diffuse hydropic degeneration which worsened to mild diffuse steatosis at the highest dose of LCFL-PTX/DXR treatment (34.7 mg/kg). Fig. 2**A–C** illustrates these findings, where **(A)** represents the control group, which is succeeded by a photo representative of the groups that received free PTX/DXR **(B)**. The arrows indicate places with apparent hydropic degeneration. Photo **(C)** represents the treatment with LCFL-PTX/DXR at the dose of 34.7 mg/kg, in which the arrows show the presence of steatosis.

Animal spleen photomicrographs are available in Fig. 2**D–F**, starting with the control group **(D)**. The image **(E)** represents the spleen of mice treated with free drugs (23.1 mg/kg), and the occurrence of congestion was observed since the red pulp was increased due to the large presence of red blood cells as indicated by the arrow. The image **(F)** shows the spleen of mice treated with free drugs (34.7 mg/kg). The presence of apoptotic corpuscles in the white pulp of the spleen, with the appearance of a "starry sky", and some corpuscles are identified by arrows. There were no changes in the lungs and kidneys of the animals treated with 20.8 mg/kg of free PTX/DXR or LCFL-PTX/DXR when compared to the control group (data not shown).

4.2.5. Electrocardiographic analysis

Due to the death of a portion of animals on the 14th day of the experiment, the analysis of the influence of treatments and time on the parameters heart rate and ST, QRS, and QTc intervals was evaluated only until 7th day. Fig. 3 shows that the time interval influenced only the LCFL-PTX/DXR treatment at the dose of 28.9 mg/kg, which was different between day 0 and 7 ($p = 0.0222$) for the QTc interval, showing its increase during this period (from 106.15 ± 10.85 ms on day 0 to 125.31 ± 19.55 ms on day 7). The prolongation of the QT interval can be seen in the electrical ECG signals also present in Fig. 3. Additionally, a statistical difference was observed between the treatments free PTX/DXR at dose of 20.8 mg/kg and LCFL-PTX/DXR treatment at dose of 28.9 mg/kg in this same parameter ($p = 0.0208$).

When comparing the influence of treatments on the same parameters mentioned on the 14th day (Fig. 4), it was possible to observe that there

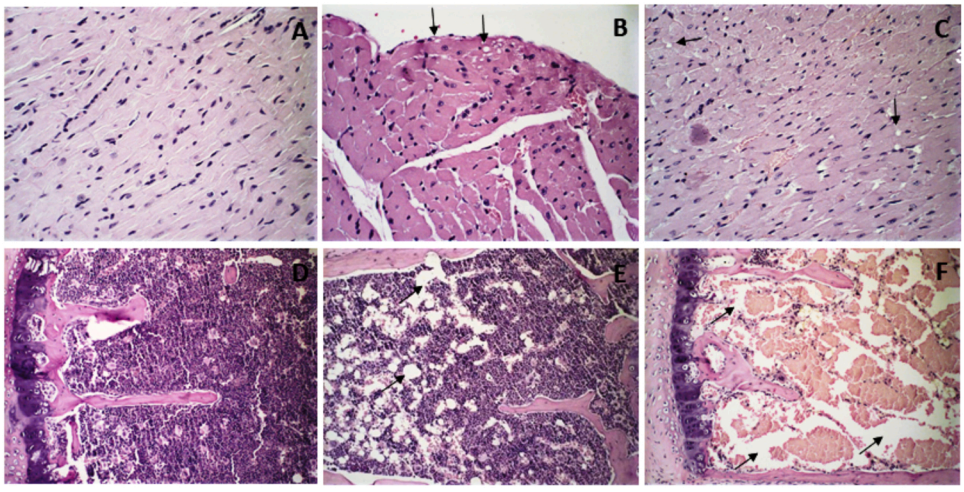

Fig. 1. Histological sections of female Balb/c mice heart and bone marrow. (A–C) Photomicrographs of the heart. (A) Represents the control group and the groups treated with all the tested doses of LCFL-PTX/DXR (20.8, 23.1, 25.4, 28.9, and 34.7 mg/kg). Cardiac fibers and cardiomyocytes without histological changes. B and C represent the groups treated with the combination of free PTX/DXR at doses of 20.8 and 23.1 mg/kg respectively. The arrows indicate the regions of cardiomyocyte vacuolization and discrete multifocal degeneration. (D–F) Bone marrow photomicrographs. D represents the control group and the groups treated with all the tested doses of free PTX/DXR (20.8 and 23.1 mg/kg) and the groups treated with LCFL-PTX/DXR (20.8, 23.1, and 25.4 mg/kg). The cells present in the medulla do not present histological changes. (E) represents the group treated with LCFL-PTX/DXR at dose of 28.9 mg/kg. The arrows indicate a reduction of cellularity in the region. (F) shows the bone marrow of mice treated with LCFL-PTX/DXR at highest dose (34.7 mg/kg). The reduction of the cellularity indicated by the arrows is even more drastic.

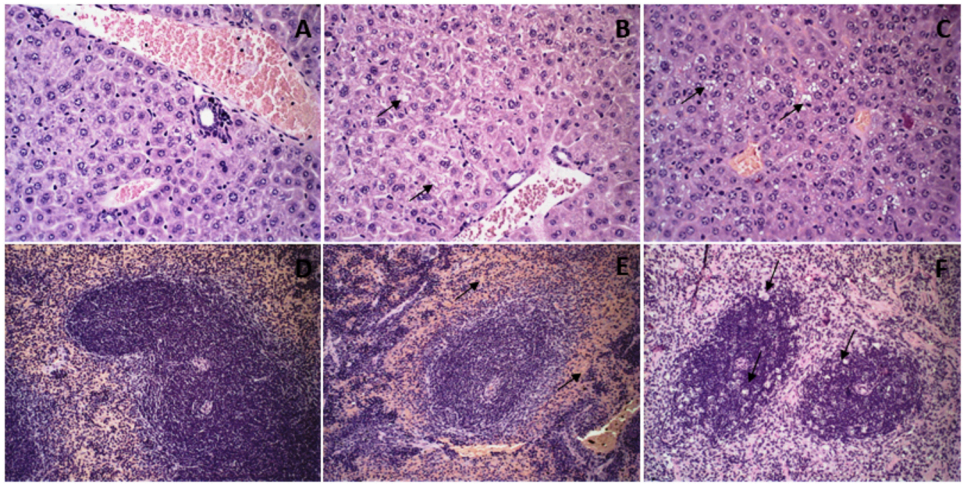

Fig. 2. Histological sections of female Balb/c mice liver and spleen. (A–C) liver photomicrographs. (A) represents the control group without histological changes in the hepatocytes. (B) represents all treatments with free PTX/DXR (20.8 and 23.1 mg/kg) and also treatments with LCFL-PTX/DXR at doses of 20.8, 23.1, 25.4, and 28.9 mg/kg. These treatments led to discrete diffuse hydropic degeneration indicated by the arrows. (C) represents the group treated with the highest dose of LCFL-PTX/DXR (34.7 mg/kg). In this specific group, multifocal steatosis started, as can be seen in the regions indicated by the arrows. (D-F) contains the spleen photomicrographs. (D) represents the control group without histological changes. (E) represents the group that received treatment with free PTX/DXR in the highest dose (23.1 mg/kg). There is an increase in the red pulp indicated by the arrow, with an agglomeration of red blood cells. (F) represents the group that received the highest dose of LCFL-PTX/DXR (34.7 mg/kg). The formation of apoptotic corpuscles can be observed as indicated by the arrow and is known as "starry sky.".

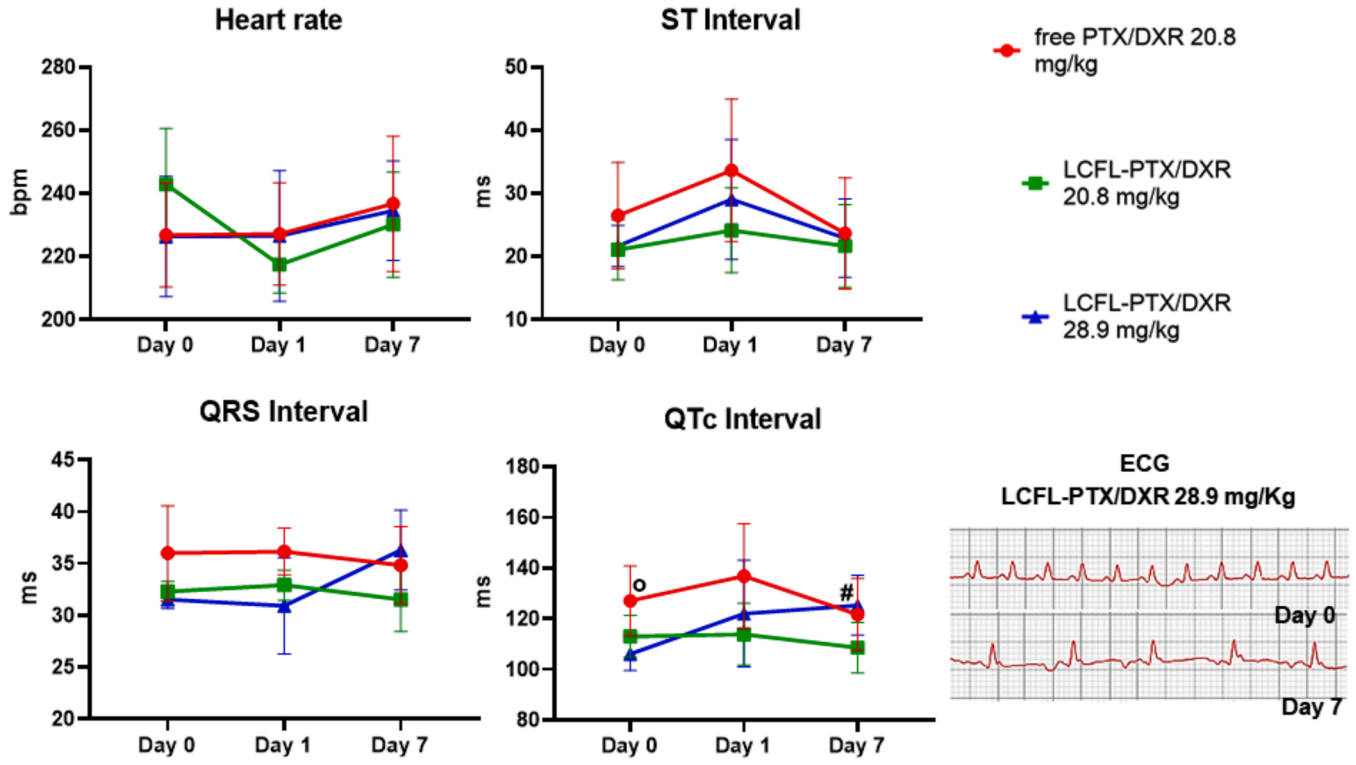

Fig. 3. Determination of cardiographic parameters for female balb/c mice after 7 days of treatment with LCFL-PTX/DXR and free PTX/DXR. The results are presented as mean ± CI. The data were evaluated by Two-way ANOVA test followed by Tukey's post-test at a significance level of 5%. # indicates a statistically significant difference for the treatment LCFL-PTX/DXR at dose of 28.9 mg/Kg between days 0 and 7. ° indicates a statistically significant difference between the groups free PTX/DXR at dose of 20.8 mg/kg and LCFLP-PTX/DXR at dose of 28.9 mg/kg on day 0.

was a statistical difference only for the QRS interval between treatments free PTX/DXR at dose of 20.8 mg/kg and LCFL-PTX/DXR at the same dose (37.00 ± 5.01 ms and 30.83 ± 2.62 ms, respectively; $p = 0.0177$). In this case, the prolongation of the QRS interval can be seen in the electrical ECG signals present in Fig. 4.

Fig. 5 shows the ratio between live animals at the end of the experiment and the total number of animals used at the beginning of the experiment. It is remarkable how the treatment with free PTX/DXR impacted the animals' survival, resulting in a higher number of deaths, when compared with the liposomal formulation for both concentrations of 20.8 and 28.9 mg/kg.

5. Discussion

LCFL-PTX/DXR proved to be of medium size and homogeneous average size distribution, being suitable for intravenous administration [6,24–26]. The encapsulation of the drugs PTX and DXR in the molar ratio (1:10) is adequate for breast cancer therapy and the zeta potential

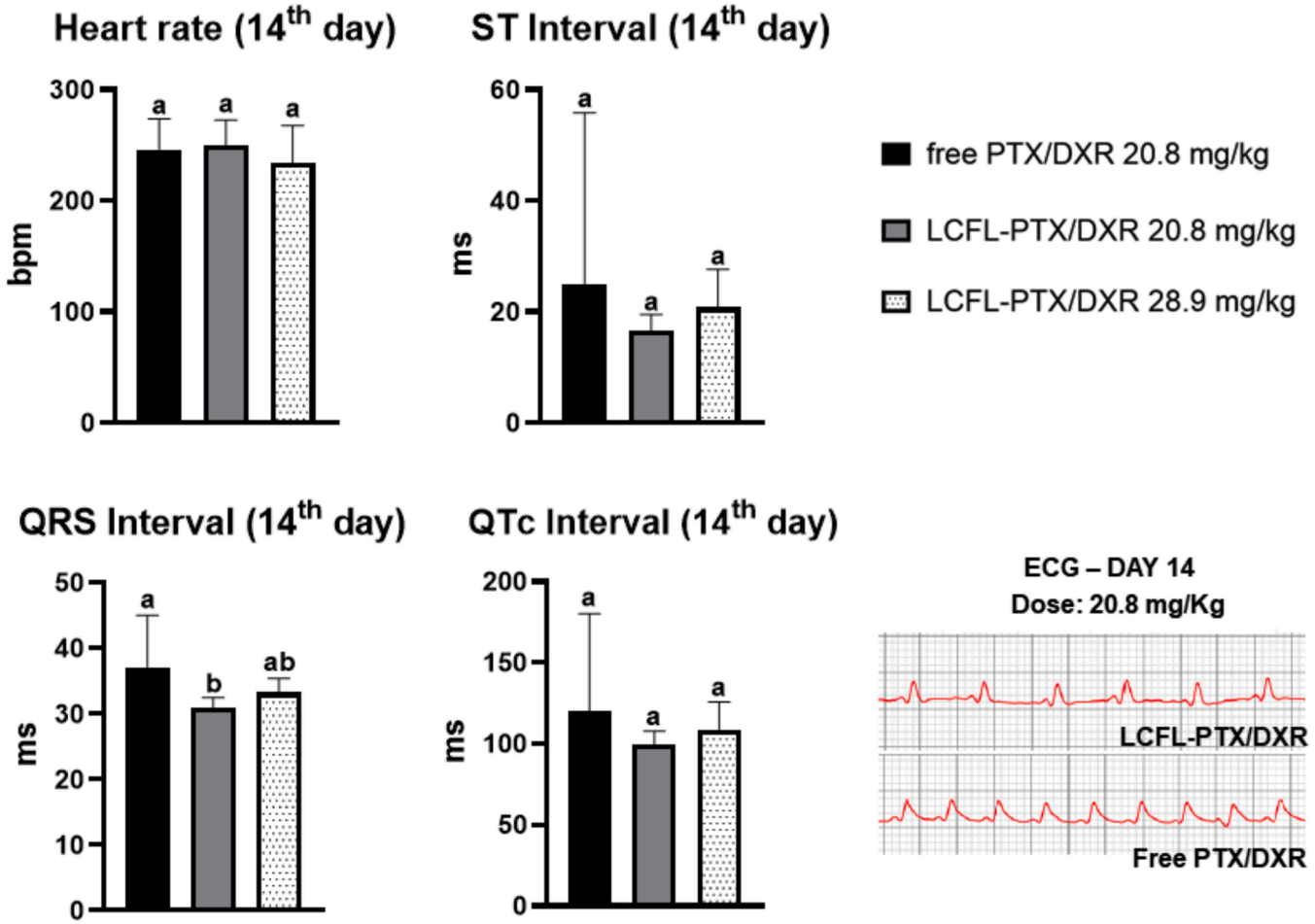

Fig. 4. Determination of cardiographic parameters for female balb/c mice after 14 days of treatment with LCFL-PTX/DXR and free PTX/DXR. The results are presented as mean ± CI. The data were evaluated by ANOVA One-way test followed by Tukey's post-test for the heart rate variable; and for the variables QRS, ST, and QTc, the Kruskal-Wallis test with Dunn's post-test was used. All tests were performed at a significance level of 5%. Different letters indicate a statistically significant difference between treatments.

close to neutrality is already expected for PEG-coated liposomes [6,26, 27]. Thus, the formulation of LCFL-PTX/DXR is suitable for toxicity studies.

The lack of data on the effect of simultaneous administration of DXR and PTX in normal tissue has led us to develop studies of toxicity of LCFL-PTX/DXR. In addition, toxicity studies are an important step when the aim is to introduce new pharmaceutical products for clinical use [14, 15]. Preclinical toxicological tests allow a scientific basis to predict the main side effects and the consequences of an overdose for further escalation in humans [16].

Initially, when evaluating only the morbidity and mortality of the animals, it is already clear that the combination of the free PTX/DXR drugs has greater toxicity compared to the liposomal formulation. This fact is true even when the dose of the liposomal formulation exceeds 8.1 mg/kg of the administration of free PTX/DXR drugs. This therapeutic benefit reduced the toxicity with a consequent increase in LD50 range. This occurs due to the different biodistribution profile of liposomes when compared to free drugs [28]. The intrinsic properties of liposomes, such as particle size, charge, and lipid composition, can produce changes in the biodistribution of drugs, leaving them prone to certain organs or tissues. In addition, lipid bilayers facilitate the transport, cell and tissue uptake, and intracellular processing of vesicles [28–30].

Given the possibility of administering free PTX/DXR only in the lowest dose of the study, due to the early mortality of mice when exposed to a dose of (23.1 mg/kg), the proof of toxic effects on organs, tissues, and systems of mice was made difficult for this group. The visualization of these effects became viable only at the highest doses of drugs, which were possible to administer only through encapsulation in liposomes. Although with slight signs of apparent toxicity, the animals that received the highest doses of LCFL-PTX/DXR remained alive and without morbidities.

Hematological evaluation showed the occurrence of mild cytopenia and an increase in the platelet production after administration of higher doses of LCFL-PTX/DXR. These findings may be due to the presence of DXR, which can interrupt red blood cell production and cause blood clotting disorders and leukopenia [21,31]. This type of toxicity affects the bone marrow, as seen in histology images. From the administration of the higher doses of LCFL-PTX/DXR, hypocellularity was detected in the medulla (sternum), which also affected the production of blood cells. For these doses, the spleen also showed signs of toxicity, evidenced as areas of apoptosis in the white pulp. This region is a zone for the production of lymphocytes, and such lesions may contribute to the cytopenia found.

In addition to renal elimination, DXR and PTX are mostly eliminated via the hepatobiliary route; therefore, the liver is an important target for injury [32–35]. Despite this, the histological analysis of the groups treated in this study, the animals that received treatments with LCFL-PTX/DXR at doses lower than LD50 range showed only small degenerative liver lesions without a significant increase in the activity of serum ALT, which is the most specific enzyme to indicate liver damage, being found predominantly in the cytoplasmic portion of hepatocytes

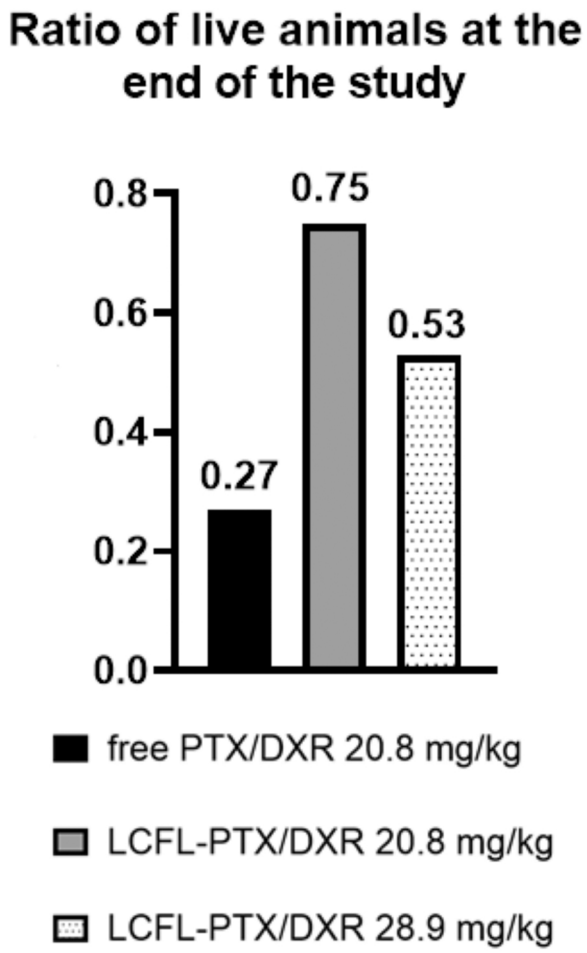

Fig. 5. Determination of the ratio of live animals at the end of study of acute toxicity. The ratio of live animals at the end of the study of acute toxicity was calculated by dividing the number of live animals at the end of the experiment by the total number of animals at the beginning of the experiment for each treatment separately.

[36]. This combination of results may indicate no or low liver toxicity induced by the liposomal formulation. The process of acute liver injury that progressed to steatosis only occurred after administration of a higher dose of LD50 [21,23]. The trend of isolated serum AST elevation that occurs in treated groups may not only be related to the increased uptake of nanosystems by the mononuclear phagocytic system, which includes the liver. In addition to the liver, AST is produced in other organs such as the heart, skeletal muscle, kidney, brain, pancreas, spleen, lung and erythrocytes [37,38]. The amount of AST in the blood is directly related to tissue damage. The high level of AST up to 300 U/L is considered non-specific [39].

Cardiotoxicity, the most well-known side effect of the use of DXR, can become serious and debilitating for patients. In our study, the administration of LCFL-PTX/DXR did not produce the appearance of cardiotoxicity. There was no structural change in cardiac tissues, such as vacuolization or hyalinization of cardiomyocytes, and the levels of the CK-MB enzyme were maintained. However, the ECG showed a small but significant difference in the QTc interval, 7 days after administration of LCFL-PTX/DXR at the dose of 28.9 mg/kg. The QT interval is a classical marker to evaluate the potential of ventricular arrhythmias for drug candidates during preclinical evaluation [40,41]. The increase in the QTc interval can be an early indicator of DXR-induced cardiotoxicity. However, the clinical consequences of QT prolongation, such as arrhythmias or sudden cardiac death, remain rare [36,42].

Another common ECG change after DXR administration is the extension of the QRS complex, which was noticed at the end of 14 days for the group that received the combination of free drugs [43]. Several reports have revealed that the QT and QRS prolongation that occurs with DXR treatment is due to the stretching of the action potentials of ventricular cardiomyocytes and is correlated with the severity of histological lesions of the heart [36,42,43]. Thus, the evaluation of the acute toxicity of the LCFL-PTX/DXR treatment allowed verification that its administration at similar doses of the combination of free PTX/DXR led to less toxic effects. Therefore, the liposomal formulation indicated to be safer, showing low or no profile of physiological and tissue changes, morbidity, and mortality, being an alternative to reduce the side effects of the breast cancer treatment.

6. Conclusion

The results of our study established that the toxicity of LCFL-PTX/DXR is lower than the combination of free PTX and DXR, proving that liposomes are capable of delivering higher doses of PTX/DXR without causing serious damage to organs and tissues, and with reduced side effects. This was reflected in the increased survival of animals treated with LCFL-PTX/DXR. Thus, regarding the toxicity, these nanosystems have significant advantages over the combination of free drugs and are a promising therapeutic platform for chemotherapy against breast cancer.

CRediT authorship contribution statement

Marjorie Coimbra Roque: Investigation, Writing – original draft. **Caroline Dohanik da Silva:** Formal analysis. **Marthin Raboch Lempek:** Investigation. **Geovanni Dantas Cassali:** Investigation. **André Luís Branco de Barros:** Investigation. **Marília Martins Melo:** Investigation. **Mônica Cristina Oliveira:** Supervision, Writing – review & editing, Project administration, Funding acquisition.

Acknowledgments

The authors would like to thank Fundação de Amparo a Pesquisa do Estado de Minas Gerais – FAPEMIG (PPM-00703-18, PPM-00387-17, CDS-APQ-01588-15 and CDS - RED-00007-14- REDE MINEIRA DE PESQUISAS EM NANOBIOTECNOLOGIA), Coordenação de Aperfeiçoamento de Pessoal de Nível Superior (CAPES) - Programa CAPES-COFECUB (Processo 88881.370874/2019-01), and Conselho Nacional de Desenvolvimento Científico e Tecnológico – CNPq (307098/2018-4, 310316/2020-0 and 429703/2018-0) for the financial support. The authors also thanks Coordenação de Aperfeiçoamento de Pessoal de Nível Superior – CAPES for supporting Marjorie Coimbra Roque with a scholarship.

Conflict of Interest

The authors declare no conflict of interest, financial or otherwise.

Appendix A. Supplementary material

Supplementary data associated with this article can be found in the online version at doi:10.1016/j.biopha.2021.112307.

References

[1] F. Bray, J. Ferlay, I. Soerjomataram, R.L. Siegel, L.A. Torre, A. Jemal, Global cancer statistics 2018: GLOBOCAN estimates of incidence and mortality worldwide for 36 cancers in 185 countries, CA Cancer J. Clin. 68 (2018) 394–424, https://doi.org/10.3322/caac.21492.

[2] A.I. Fraguas-Sánchez, A. Fernández-Carballido, R. Simancas-Herbada, C. Martin-Sabroso, A.I. Torres-Suárez, CBD loaded microparticles as a potential formulation to improve paclitaxel and doxorubicin-based chemotherapy in breast cancer, Int. J. Pharm. 574 (2020), 118916, https://doi.org/10.1016/j.ijpharm.2019.118916.

[3] C. Meyer, C. Bailleux, E. Chamorey, R. Schiappa, Y. Delpech, M. Dejode, Y. Fouché, J. Haudebourg, E. Barranger, Factors involved in delaying initiation of adjuvant

chemotherapy after breast cancer surgery, Clin. Breast Cancer (2021), https://doi.org/10.1016/j.clbc.2021.05.007.
[4] Y. Wang, J. Wang, L. Yang, W. Wei, B. Sun, K. Na, Y. Song, H. Zhang, Z. He, J. Sun, Y. Wang, Redox dual-responsive paclitaxel-doxorubicin heterodimeric prodrug self-delivery nanoaggregates for more effective breast cancer synergistic combination chemotherapy, Nanomed. Nanotechnol. Biol. Med. 21 (2019), 102066, https://doi.org/10.1016/j.nano.2019.102066.
[5] C. Feng, H. Zhang, J. Chen, S. Wang, Y. Xin, Y. Qu, Q. Zhang, W. Ji, F. Yamashita, M. Rui, X. Xu, Ratiometric co-encapsulation and co-delivery of doxorubicin and paclitaxel by tumor-targeted lipodisks for combination therapy of breast cancer, Int. J. Pharm. 560 (2019) 191–204, https://doi.org/10.1016/j.ijpharm.2019.02.009.
[6] M.C. Roque, M.S. Franco, J.M.C. Vilela, M.S. Andrade, A.L.B. de Barros, E.A. Leite, M.C. Oliveira, Development of long-circulating and fusogenic liposomes co-encapsulating paclitaxel and doxorubicin in synergistic ratio for the treatment of breast cancer, Curr. Drug Deliv. 16 (2019) 829–838, https://doi.org/10.2174/1567201816666191016112717.
[7] J. Yu, Y. Wang, S. Zhou, J. Li, J. Wang, D. Chi, X. Wang, G. Lin, Z. He, Y. Wang, Remote loading paclitaxel–doxorubicin prodrug into liposomes for cancer combination therapy, Acta Pharm. Sin. B 10 (2020) 1730–1740, https://doi.org/10.1016/j.apsb.2020.04.011.
[8] T.-C. Chou, N. Martin, CompuSyn for Drug Combinations and for General Dose-Effect Analysis User's Guide, 2005, pp. 1–68. ⟨www.combosyn.com⟩ with.
[9] T.C. Chou, Theoretical basis, experimental design, and computerized simulation of synergism and antagonism in drug combination studies, Pharmacol. Rev. 58 (2006) 621–681, https://doi.org/10.1124/pr.58.3.10.
[10] M.S. Franco, M.C. Oliveira, Liposomes co- encapsulating anticancer drugs in synergistic ratios as an approach to promote increased efficacy and greater safety, Anticancer. Agents Med. Chem. 19 (2018) 17–28, https://doi.org/10.2174/1871520618666180420170124.
[11] H. Baabur-Cohen, L.I. Vossen, H.R. Krüger, A. Eldar-boock, E. Yeini, N. Landa-Rouben, G. Tiram, S. Wedepohl, E. Markovsky, J. Leor, M. Calderón, R. Satchi-Fainaro, In vivo comparative study of distinct polymeric architectures bearing a combination of paclitaxel and doxorubicin at a synergistic ratio, J. Control. Release 257 (2016) 118–131, https://doi.org/10.1016/j.jconrel.2016.06.037.
[12] P.G. Tardi, R.C. Gallagher, S. Johnstone, N. Harasym, M. Webb, M.B. Bally, L. D. Mayer, Coencapsulation of irinotecan and floxuridine into low cholesterol-containing liposomes that coordinate drug release in vivo, Biochim. Biophys. Acta - Biomembr. 1768 (2007) 678–687, https://doi.org/10.1016/j.bbamem.2006.11.014.
[13] M.S. Franco, M.C. Oliveira, Ratiometric drug delivery using non-liposomal nanocarriers as an approach to increase efficacy and safety of combination chemotherapy, Biomed. Pharmacother. 96 (2017) 584–595, https://doi.org/10.1016/j.biopha.2017.10.009.
[14] C.M. Liu, C.H. Chang, Y.J. Chang, C.W. Hsu, L.C. Chen, H.L. Chen, C.L. Ho, C.Y. Yu, T.J. Chang, T.C. Chiang, T.W. Lee, Preliminary evaluation of acute toxicity of 188Re-BMEDA-liposome in rats, J. Appl. Toxicol. 30 (2010) 680–687, https://doi.org/10.1002/jat.1541.
[15] S.Y. Liu, C.H. Chang, T.W. Lee, Single dose acute toxicity testing for N,N-bis(2-mercaptoethyl)-N′,N′ diethylethylenediamine in beagles, Regul. Toxicol. Pharmacol. 69 (2014) 217–225, https://doi.org/10.1016/j.yrtph.2014.04.001.
[16] K. Chapman, S. Creton, H. Kupferschmidt, G.R. Bond, M.F. Wilks, S. Robinson, The value of acute toxicity studies to support the clinical management of overdose and poisoning: a cross-discipline consensus, Regul. Toxicol. Pharmacol. 58 (2010) 354–359, https://doi.org/10.1016/j.yrtph.2010.07.003.
[17] M.R. Rasch, Y. Yu, C. Bosoy, B.W. Goodfellow, B.A. Korgel, Chloroform-enhanced incorporation of hydrophobic gold nanocrystals into dioleoylphosphatidylcholine (DOPC) vesicle membranes, Langmuir 11 (2013) 12971–12981, https://doi.org/10.1021/la302740j.
[18] L.O.F. Monteiro, R.S. Fernandes, C.M.R. Oda, S.C. Lopes, D.M. Townsend, V. N. Cardoso, M.C. Oliveira, E.A. Leite, D. Rubello, A.L.B. de Barros, Paclitaxel-loaded folate-coated long circulating and pH-sensitive liposomes as a potential drug delivery system: a biodistribution study, Biomed. Pharmacother. 97 (2018) 489–495, https://doi.org/10.1016/j.biopha.2017.10.135.
[19] M.S. Oliveira, S.V. Mussi, D.A. Gomes, M.I. Yoshida, F. Frezard, V.M. Carregal, L.A. M. Ferreira, α-Tocopherol succinate improves encapsulation and anticancer activity of doxorubicin loaded in solid lipid nanoparticles, Colloids Surf. B Biointerfaces 140 (2016) 246–253, https://doi.org/10.1016/j.colsurfb.2015.12.019.
[20] OECD, Test No. 423: Acute Oral Toxicity – Acute Toxic Class Method, Oecd Guidel. Test. Chem., 2001, pp. 1–14. ⟨https://doi.org/10.1787/9789264071001-en⟩.
[21] J. de Oliveira Silva, S.E.M. Miranda, E.A. Leite, A. de Paula Sabino, K.B.G. Borges, V.N. Cardoso, G.D. Cassali, A.G. Guimarães, M.C. Oliveira, A.L.B. de Barros, Toxicological study of a new doxorubicin-loaded pH-sensitive liposome: a preclinical approach, Toxicol. Appl. Pharmacol. 352 (2018) 162–169, https://doi.org/10.1016/j.taap.2018.05.037.
[22] D.R. Abernethy, D.L. Wesche, J.T. Barbey, C. Ohrt, S. Mohanty, J.C. Pezzullo, B. G. Schuster, Stereoselective halofantrine disposition and effect: concentration-related QTc prolongation, Br. J. Clin. Pharm. 51 (2001) 231–237, https://doi.org/10.1046/j.1365-2125.2001.00351.x.
[23] K. Razavi-Azarkhiavi, A.H. Jafarian, K. Abnous, B.M. Razavi, K. Shirani, M. Zeinali, M.R. Jaafari, G. Karimi, The comparison of biodistribution, efficacy and toxicity of two PEGylated liposomal doxorubicin formulations in mice bearing C-26 colon carcinoma: a preclinical study, Drug Res. 66 (2016) 330–336, https://doi.org/10.1055/s-0035-1569447.
[24] S. Barua, S. Mitragotri, Challenges associated with penetration of nanoparticles across cell and tissue barriers: a review of current status and future prospects, Nano Today 9 (2014) 223–243, https://doi.org/10.1016/j.nantod.2014.04.008.
[25] P.I. Siafaka, N. Üstündağ Okur, E. Karavas, D.N. Bikiaris, Surface modified multifunctional and stimuli responsive nanoparticles for drug targeting: current status and uses, Int. J. Mol. Sci. 17 (2016) 1–40, https://doi.org/10.3390/ijms17091440.
[26] M.S. Franco, M.C. Roque, M.C. Oliveira, Short and long-term effects of the exposure of breast cancer cell lines to different ratios of free or co-encapsulated liposomal paclitaxel and doxorubicin, Pharmaceutics 11 (2019), https://doi.org/10.3390/pharmaceutics11040178.
[27] S.K. Ramadass, N.V. Anantharaman, S. Subramanian, S. Sivasubramanian, B. Madhan, Paclitaxel/epigallocatechin gallate coloaded liposome: a synergistic delivery to control the invasiveness of MDA-MB-231 breast cancer cells, Colloids Surf. B Biointerfaces 125 (2015) 65–72, https://doi.org/10.1016/j.colsurfb.2014.11.005.
[28] Y. Wang, D.W. Grainger, Lyophilized liposome-based parenteral drug development: reviewing complex product design strategies and current regulatory environments, Adv. Drug Deliv. Rev. 151–152 (2019) 56–71, https://doi.org/10.1016/j.addr.2019.03.003.
[29] S. Hua, S.Y. Wu, The use of lipid-based nanocarriers for targeted pain therapies, Front. Pharmacol. 4 (NOV) (2013) 1–7, https://doi.org/10.3389/fphar.2013.00143.
[30] N. Monteiro, A. Martins, R.L. Reis, N.M. Neves, Liposomes in tissue engineering and regenerative medicine, J. R. Soc. Interface 11 (2014), 20140459, https://doi.org/10.1098/rsif.2014.0459.
[31] M.M. Khiavi, E. Anvari, H. Hamishehkar, K. Abdal, Assessment of the blood parameters, cardiac and liver enzymes in oral squamous cell carcinoma following treated with injectable doxorubicin-loaded nano-particles, Asian Pac. J. Cancer Prev. 20 (2019) 1973–1977, https://doi.org/10.31557/APJCP.2019.20.7.1973.
[32] X. Su, Z. Wang, L. Li, M. Zheng, C. Zheng, P. Gong, P. Zhao, Y. Ma, Q. Tao, L. Cai, Lipid-polymer nanoparticles encapsulating doxorubicin and 2′-deoxy-5-azacytidine enhance the sensitivity of cancer cells to chemical therapeutics, Mol. Pharm. 10 (2013) 1901–1909, https://doi.org/10.1021/mp300675c.
[33] R.X. Zhang, H.L. Wong, H.Y. Xue, J.Y. Eoh, X.Y. Wu, Nanomedicine of synergistic drug combinations for cancer therapy – strategies and perspectives, J. Control. Release 240 (2016) 489–503, https://doi.org/10.1016/j.jconrel.2016.06.012.
[34] S. Sritharan, N. Sivalingam, A comprehensive review on time-tested anticancer drug doxorubicin, Life Sci. 278 (2021), 119527, https://doi.org/10.1016/j.lfs.2021.119527.
[35] M. Ashrafizadeh, S. Mirzaei, F. Hashemi, A. Zarrabi, A. Zabolian, H. Saleki, S. O. Sharifzadeh, L. Soleymani, S. Daneshi, K. Hushmandi, H. Khan, A.P. Kumar, A. R. Aref, S. Samarghandian, New insight towards development of paclitaxel and docetaxel resistance in cancer cells: EMT as a novel molecular mechanism and therapeutic possibilities, Biomed. Pharmacother. 141 (2021), 111824, https://doi.org/10.1016/j.biopha.2021.111824.
[36] H.S. Mohammed, E.N. Hosny, Y.A. Khadrawy, M. Magdy, Y.S. Attia, O.A. Sayed, M. AbdElaal, Protective effect of curcumin nanoparticles against cardiotoxicity induced by doxorubicin in rat, Biochim. Biophys. Acta - Mol. Basis Dis. 1866 (2020), 165665, https://doi.org/10.1016/j.bbadis.2020.165665.
[37] Z. Mohammed-Ali, D. Brinc, V. Kulasingam, R. Selvaratnam, Defining appropriate utilization of AST testing, Clin. Biochem. 79 (2020) 75–77, https://doi.org/10.1016/j.clinbiochem.2020.02.006.
[38] G. Ndrepepa, S. Holdenrieder, S. Cassese, E. Xhepa, M. Fusaro, K.L. Laugwitz, H. Schunkert, A. Kastrati, Aspartate aminotransferase and mortality in patients with ischemic heart disease, Nutr. Metab. Cardiovasc. Dis. 30 (2020) 2335–2342, https://doi.org/10.1016/j.numecd.2020.07.033.
[39] A. Rasool, M. Zulfajri, A. Gulzar, M.M. Hanafiah, S.A. Unnisa, M. Mahboob, In vitro effects of cobalt nanoparticles on aspartate aminotransferase and alanine aminotransferase activities of wistar rats, Biotechnol. Rep. 26 (2020), https://doi.org/10.1016/j.btre.2020.e00453.
[40] X. Xia, R. Wu, S. An, R. Li, S. Mcpherson, Comparison of different QTc formulae for correction of QT interval in cynomolgus monkeys, J. Pharmacol. Toxicol. Methods 99 (2019), https://doi.org/10.1016/j.vascn.2019.05.147.
[41] S.W. Rabkin, E. Szefer, D.J.S. Thompson, A new QT interval correction formulae to adjust for increases in heart rate, JACC Clin. Electrophysiol. 3 (2017) 756–766, https://doi.org/10.1016/j.jacep.2016.12.005.
[42] T. Kinoshita, H. Yuzawa, K. Natori, R. Wada, S. Yao, K. Yano, K. Akitsu, H. Koike, M. Shinohara, T. Fujino, H. Shimada, T. Ikeda, Early electrocardiographic indices for predicting chronic doxorubicin-induced cardiotoxicity, J. Cardiol. 77 (2021) 388–394, https://doi.org/10.1016/j.jjcc.2020.10.007.
[43] M. Khalilzadeh, A. Abdollahi, F. Abdolahi, A.H. Abdolghaffari, A.R. Dehpour, F. Jazaeri, Protective effects of magnesium sulfate against doxorubicin induced cardiotoxicity in rats, Life Sci. 207 (2018) 436–441, https://doi.org/10.1016/j.lfs.2018.06.022.